2022 IEEE International Conference on Intelligent Transportation Systems (ITSC 2022)
Accepted paper. Accepted June 2022

Obstacle Avoidance Control Based on Nonlinear MPC for All Wheel Driven In-Wheel EV in Steering Failure

Mizuho Aoki[1], Kohei Honda[1], Hiroyuki Okuda[1], Tatsuya Suzuki[1], Akira Ito[1], and Daisuke Nagasaka[2]

***Abstract*— Self-driving electric vehicles are becoming popular, and the demand for safer driving systems is increasing. Electric vehicles equipped with in-wheel motors (EV-IWM) can independently control the torque generated by each of the four wheels. This strong feature makes them suitable for advanced collision avoidance in emergencies. To handle the many control outputs needed to control such vehicles, most conventional research works used rule-based and hierarchical controllers. However, such constraints for making the control easier are considered to degrade the performance.**

This study presents nonlinear model predictive control (NMPC) -based method that can consider the detailed vehicle dynamics without overall linear approximation to maximize the control performance. The effectiveness of our proposed scheme is demonstrated by simulating obstacle avoidance in the case of steering failure. The recently published proximal averaged Newton-type method for optimal control (PANOC) is used as an optimization solver that reduces the computation time and enables real-time control.

The obstacle avoidance task is one example of the utilization of control redundancy. In the future, other tasks such as energy-efficient driving or improving riding comfort are expected to be realized with our proposed scheme.

I. INTRODUCTION

Autonomous driving technology has been developed in recent years. As technology becomes more widely used, more sophisticated safety features are required. There are several components of autonomous driving technology, such as recognition, decision-making, and control. Among them, vehicle control is especially important in terms of ensuring safety in emergencies by avoiding obstacles.

[1] M. Aoki, K. Honda, H. Okuda, T. Suzuki, and A.Ito belong to Nagoya University, Furo-cho, Chikusa-ku, Nagoya, Aichi, Japan, E-mail: mizuhoaoki1998@gmail.com

[2] D.Nagasaka belongs to J-QuAD DYNAMICS Inc., Kariya, Japan, E-mail: daisuke.nagasaka.j5u@j-quad.global

Electric vehicles equipped with in-wheel motors (EV-IWM) can independently control the torque of each of the four wheels (See Fig.1), which enables them to achieve motion control that is not possible with conventional steer controlled vehicles. EV-IWM is a redundant system because there are several ways to turn vehicles by controlling the steering input and tuning the balance of generated wheel torques. Redundancy not only contributes to the flexibility of the motion control but also the safety in the sense that the vehicle can change course even if the steer operation does not work. However, because of the redundant and multiple control outputs, torque distribution control is difficult. In the past, direct yaw-moment control (DYC) was proposed as a method focused on the control of yaw-moment, and rule-based approaches were used [1] [2] [3]. Although it works stably, there is a concern that the performance is not maximized owing to the constraints. Optimization-based methods are effective to solve this issue. Controllers such as the linear quadratic regulator (LQR) [4] [5] and the linear model predictive controller (LMPC) [6] [7] have been proposed in the past, but linearized models still reduce the performance because of approximation effects.

The nonlinear model predictive control (NMPC) is a promising method for dealing with complex control systems. The advantages of NMPC are 1. applicable to nonlinear multiple-input and multiple-output (MIMO) systems, 2. ability to consider constraints, 3. flexibility to set multiple achievement goals by setting an evaluation function to be optimized appropriately. For the above reasons, there is much literature which approaches path tracking [8] and obstacle avoidance control [9] [10] using NMPC. In most cases, approximated models such as Dynamic Bicycle Model [11] [12] are used to express vehicle behavior to easily achieve

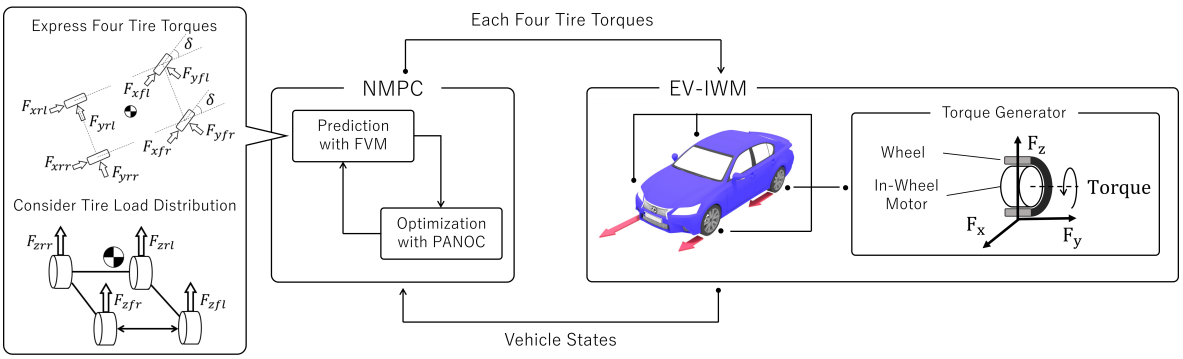

Fig. 1. Overview of the System Architecture

TABLE I

DEFINITION OF VARIABLES

Variable	Definition	Value [Unit]
${}^{G}p_x, {}^{G}p_y$	X/Y axis of Global frame	- [m]
${}^{B}p_x, {}^{B}p_y$	X/Y axis of Base frame	- [m]
${}^{F}p_x, {}^{F}p_y$	X/Y axis of Frenet-Serret frame	- [m]
θ_F	Yaw Angle between the Ref. Path	- [rad]
β	Slip Angle of Vehicle Body	- [rad]
γ	Yaw Rate of Vehicle Body	- [rad/s]
δ	Front Wheel Angle	- [rad]
T	Torque generated by a tire.	- [Nm]
ρ_{ref}	Curvature of Ref. Path	- [m^{-1}]
θ_{ref}	Yaw Angle of the Ref. in Global Frame	- [rad]
${}^{B}v_y$	Vehicle Longitudinal Velocity	- [m/s]
V	Vehicle velocity	- [m/s]
a_x	Longitudinal acceleration	- [$\mathrm{m/s^2}$]
a_y	Lateral acceleration	- [$\mathrm{m/s^2}$]
l_f	Distance from CoG to the Front Axle	1.04 [m]
l_r	Distance from CoG to the Rear Axle	1.56 [m]
d_f, d_r	Front / Rear tread	2.082 [m]
m	Mass of vehicle body	1270 [kg]
I_z	Inertia of vehicle yaw moment	1343 [$\mathrm{kgm^2}$]
H	Height of CoG	0.540[m]
R	Tire radius	0.3[m]
e, f	Tire parameter coefficients	4.15, 855.0
g	Gravitational acceleration	9.807 [$\mathrm{m/s^2}$]

CoG: center of gravity

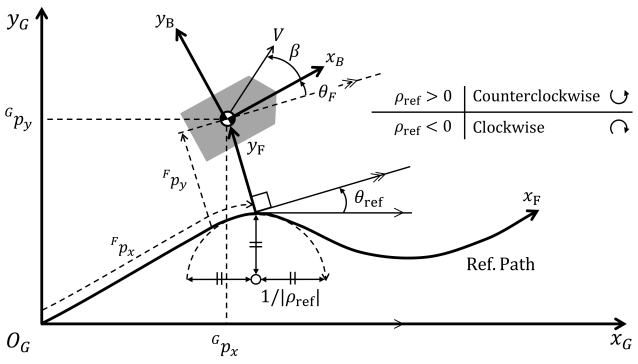

Fig. 2. Geometrical Relationship Between the Coordinates

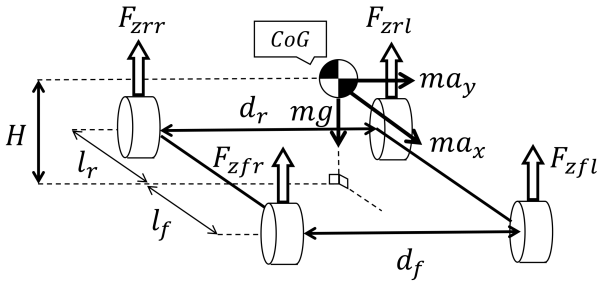

Fig. 3. Tire Load

autonomous driving with NMPC. Recently, however, some literature was successful in handling detailed vehicle models considering the forces on all four tires [13] [14].

This paper presents an NMPC controller (Fig.1) for obstacle avoidance using EV-IWM. Our proposed method incorporates a full vehicle model into NMPC instead of using a rule-based torque distributor and linearized vehicle dynamics model as in the conventional methods. As a result, it is possible to achieve optimal obstacle avoidance behavior with flexibility in using redundant control outputs. In particular, we demonstrate that obstacle avoidance is possible by using only tire torque for control, even in case of steering failure.

Our scheme also has the following features that make it easy to use in practical applications. 1. the proximal averaged Newton-type method for optimal control (PANOC) [15] is introduced as an optimization problem solver to reduce computation time and achieve real-time control. 2. Modify the vehicle dynamics model and use wheel torques for control output instead of slip rates for easier practical use, because a torque generated by a motor can be easily calculated from the input electric current value. 3. Introduce time-state control [16] [17] to express obstacle locations as relative positions to the reference trajectory.

II. FULL VEHICLE MODEL IN NMPC

To achieve high-performance obstacle avoidance, a nonlinear full vehicle model [13] is introduced as a prediction model of NMPC. In the following, this vehicle model is derived using the frenet-serret coordinate system shown in Fig.2. Please refer to [8] for details. All definitions of the variables in the following are shown in Table. I.

First, assuming that the road surface is flat, the load on each wheel F_{z**} can be calculated as follows:

$$F_{zfl} = \frac{m_f g}{2} - \frac{mHa_x}{2l} - \frac{m_f H a_y}{d_f}, \tag{1}$$

$$F_{zfr} = \frac{m_f g}{2} - \frac{mHa_x}{2l} + \frac{m_f H a_y}{d_f}, \tag{2}$$

$$F_{zrl} = \frac{m_r g}{2} + \frac{mHa_x}{2l} - \frac{m_r H a_y}{d_r}, \tag{3}$$

$$F_{zrr} = \frac{m_r g}{2} + \frac{mHa_x}{2l} + \frac{m_r H a_y}{d_r}, \tag{4}$$

where, $m_f = ml_r/(l_f + l_r)$, $m_l = ml_f/(l_f + l_r)$ and the definitions of the the variables are shown in Table. I. Next, each tire slip angle is derived from the geometric relationships by

$$\beta_{fl} = \tan^{-1}\left(\frac{V\sin\beta + l_f\gamma}{V\cos\beta - \frac{d_f\gamma}{2}}\right) - \delta, \tag{5}$$

$$\beta_{fr} = \tan^{-1}\left(\frac{V\sin\beta + l_f\gamma}{V\cos\beta + \frac{d_f\gamma}{2}}\right) - \delta, \tag{6}$$

$$\beta_{rl} = \tan^{-1}\left(\frac{V\sin\beta - l_r\gamma}{V\cos\beta - \frac{d_r\gamma}{2}}\right), \tag{7}$$

$$\beta_{rr} = \tan^{-1}\left(\frac{V\sin\beta - l_r\gamma}{V\cos\beta + \frac{d_r\gamma}{2}}\right). \tag{8}$$

The lateral and longitudinal forces generated by each tire are given by

$$F_{y**} = -(e \cdot F_{z**} + f)\beta_{**} \tag{9}$$

$$F_{x**} = T_{**}/R \tag{10}$$

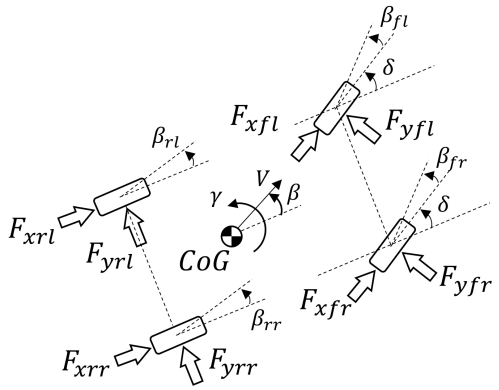

Fig. 4. Four Wheel Model

where, ** is replaced by the indices fl (front-left), fr (front-right), rl (rear-left), and rr (rear-right) indicating each tire, respectively. e, f are parameters for expressing cornering stiffness as a function of F_{z**}, and R is a tire radius.

The state vector of the MPC controller for EV-IWM is

$$x = [{}^F p_y, \theta_F, V, \gamma, \beta, a_x, a_y], \tag{11}$$

where the state equations for the state variables are given as follows:

$$\mathrm{d}{}^F p_y/\mathrm{d}t = V\cos\beta\sin\theta_F + V\sin\beta\cos\theta_F, \tag{12}$$

$$\mathrm{d}\theta_F/\mathrm{d}t = \gamma - {}^{\dot{F}}p_x\rho_{ref}, \tag{13}$$

$$\mathrm{d}{}^F p_x/\mathrm{d}t = \frac{V\cos\beta\cos\theta_F - V\sin\beta\sin\theta_F}{1-\rho_{ref}^F p_y}, \tag{14}$$

$$\mathrm{d}V/\mathrm{d}t = a_y\sin\beta + a_x\cos\beta, \tag{15}$$

$$\mathrm{d}\beta/\mathrm{d}t = (a_y\cos\beta - a_x\sin\beta)/V - \gamma, \tag{16}$$

$$\begin{aligned}\mathrm{d}\gamma/\mathrm{d}t = {} & (l_f((F_{xfl}+F_{xfr})\sin\delta) + (F_{yfl}+F_{yfr})\cos\delta) \\ & + d_f(F_{xfr}-F_{xfl})\cos\delta)/2 + d_f(F_{yfl}-F_{yfr})\sin\delta/2 \\ & - l_r(F_{yrl}+F_{yrr}) + d_r(F_{xrr}-F_{xrl})/2)/I_{zz},\end{aligned} \tag{17}$$

Because it is impossible to obtain all state variables at once from the equations, a_x and a_y are taken from the previously given values. The derivatives of a_x and a_y are obtained by assuming a first-order delay system. It is unlikely to cause practical problems if the time delay T_{delay} is small enough. $T_{\mathrm{delay}} = 0.05[s]$ is used in this study.

$$\begin{aligned}\tilde{a}_x = {} & \frac{1}{m}(-F_{yfl}\sin\delta - F_{yfr}\sin\delta \\ & + F_{xfl}\cos\delta + F_{xfr}\cos\delta + F_{xrl} + F_{xrr})\end{aligned} \tag{18}$$

$$\begin{aligned}\tilde{a}_y = {} & \frac{1}{m}(F_{yfl}\cos\delta + F_{yrl}\cos\delta \\ & + F_{yrl} + F_{yrr} + F_{xfl}\sin\delta + F_{xfr}\sin\delta)\end{aligned} \tag{19}$$

$$\mathrm{d}a_x/\mathrm{d}t = \frac{1}{T_{\mathrm{delay}}}(\tilde{a}_x - a_x) \tag{20}$$

$$\mathrm{d}a_y/\mathrm{d}t = \frac{1}{T_{\mathrm{delay}}}(\tilde{a}_y - a_y) \tag{21}$$

This study uses time-state control [16] [17] to simply describe the location of obstacles. Let ξ be the state variable, then the conversion of the time-axis state control is expressed by the following chain rule.

$$\frac{d\xi}{d^F p_x} = \frac{d\xi}{dt}\frac{dt}{d^F p_x} = \frac{d\xi}{dt}\Big/\frac{d^F p_x}{dt} \tag{22}$$

III. Vehicle Controller based on NMPC

A. Formulation of optimization problem for NMPC

Since the driving torque input for all four motors and the steering angle can be controlled independently, the all-wheel-driven (AWD) vehicle is over-actuated and redundant. This study utilizes model predictive control to determine the distribution of the driving force for each tire and steering angle directly. In the case of applying the controller to a real system, it is necessary for the in-wheel motors to follow the given torque commands.

The optimization problem solved in each control interval in NMPC is formulated as follows, putting ${}^F p_x$ with s for the convenience of visibility,

Given: (23)

$$\hat{x}(0|s) = x(s) = [{}^F p_y, \theta_F, V, \gamma, \beta, a_x, a_y], \tag{24}$$

$$x_{\mathrm{ref}} = [0, 0, V_{\mathrm{ref}}, 0, 0, 0, 0], \tag{25}$$

$$S_f,\ Q,\ R,\ ,R',\ C_x,\ C_y,\ C_r,\ N_{obj},\ W_{obj},\ \delta_{max},\ T_{max},$$

Find:

$$\begin{aligned}&\hat{x}(k|s), \quad \forall k \in \{1,\ldots,N\}, \\ &\hat{u}(k|s) = [\hat{\delta}(k|s), \hat{T}_{fl}(k|s), \hat{T}_{fr}(k|s), \hat{T}_{rl}(k|s), \hat{T}_{rr}(k|s)]^T, \\ &\forall k \in \{0,\ldots,N-1\},\end{aligned} \tag{26}$$

Which minimize:

$$J = \Phi(\hat{x}(N|s)) + \sum_{k=0}^{N-1} L(\hat{x}(k|s), \hat{u}(k|s))\Delta s, \tag{27}$$

$$\Phi(\hat{x}(N|s)) = \frac{1}{2}(\hat{x}(N|s) - x_{\mathrm{ref}})^T S_f (\hat{x}(N|s) - x_{\mathrm{ref}}), \tag{28}$$

$$\begin{aligned}L(\hat{x}(k|s)) = {} & \frac{1}{2}(\hat{x}(k|s) - x_{\mathrm{ref}})^T Q(\hat{x}(k|s) - x_{\mathrm{ref}}) \\ & + \hat{u}(k|s)^T R\hat{u}(k|s) \\ & + (\hat{u}(k|s) - \hat{u}(k-1|s))^T R' (\hat{u}(k|s) - \hat{u}(k-1|s)) \\ & + P(\hat{x}(k|s)),\end{aligned} \tag{29}$$

$$P(\hat{x}(k|s)) = \sum_{j=1}^{N_{obj}} \frac{W_{obj}}{({}^F p_x(k|s) - C_{jx})^2 + ({}^F p_y(k|s) - C_{jy})^2}, \tag{30}$$

Subject to:

$$\hat{x}(k+1|s) = \hat{x}(k|s) + \frac{\mathrm{d}x}{\mathrm{d}s}\Delta s, \tag{31}$$

$$|\delta| < \delta_{max}, \tag{32}$$

$$|T_{fl}|, |T_{fr}|, |T_{rl}|, |T_{rr}| < T_{max}, \tag{33}$$

$$C_r^2 - \left((p_{x**} - C_{jx})^2 + (p_{y**} - C_{jy})^2\right) < 0, \tag{34}$$

where $x(s)$ is a state vector defined by (11), S_f, Q, R and R' are the weight matrices. J is the cost function to be minimized, which consists of stage cost L, terminal cost Φ, and potential field penalty P. See Table.I for the definitions of the variables.

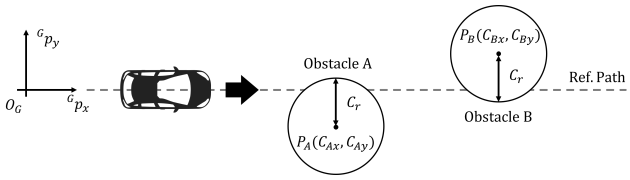

Fig. 5. Obstacle Avoidance Situation

Hard constraints (34) work to guarantee that the vehicle never collides with obstacles. Moreover, the artificial potential field (APF) [18] added to the stage cost allow the vehicle to drive keeping certain distances away from obstacles. W_{obj} in Eq.(30) is a parameter that determines the level of influence of obstacles, and the value shown in Table.II is used in this study.

Note that ** indicates every four points of the vehicle body rectangle. It is assumed that the vehicle does not collide if all of the four points are outside the circular areas of the obstacles.

B. Implementation of NMPC

One of the difficulties when applying NMPC is how to solve the optimization problem in real-time. This study uses the proximal averaged Newton-type method for optimal control (PANOC) [15] as an optimization solver. It is a combination of the proximal gradient method and quasi-Newton method so that most optimization problems of NMPC are calculated much faster than other methods such as sequential quadratic programming and the interior point method. We use OpEn [19], a wrapper of PANOC for implementation. PANOC is a method for unconstrained optimization, However, OpEn can handle constraints using the penalty function method [20]. For this reason, the constraints in eqs.(32)–(34) are handled as penalty functions.

IV. OBSTACLE AVOIDANCE SIMULATION

In this section, two types of simulations are implemented. The first one (Section. IV-B) is an obstacle avoidance task using both steer and each four tire torque, and the other one (Section. IV-C) is emergency avoidance behavior in the case of a steering failure. The full vehicle model (Section. II) in the Global frame is used as a simulator with the assumption that the time delay is 0 [s] in following the reference value of torque generation.

A. Problem settings

The target task is set as obstacle avoidance as shown in Fig.5 in the simulation. The vehicle tries to follow the given straight reference path as closely as possible while avoiding two circular obstacles. The radius C_r and positions of the two obstacles (C_{*x}, C_{*y}) are defined as follows.

$$C_r = 2.0 \text{ [m]}$$
$$P_A(C_{Ax}, C_{Ay}) = (10 \text{ [m]}, -1.5 \text{ [m]})$$
$$P_B(C_{Bx}, C_{By}) = (25 \text{ [m]}, 1.5 \text{ [m]})$$

TABLE II
COMMON PARAMETERS IN SIMULATIONS

Control interval	0.05 [s]
Δt	0.05 [m]
N	50 [step]
$V_{\rm ref}$	6.95 [m/s] (25 [km/h])
$W_{\rm obj}$	45.0 [-]

The initial values of the state variables is $x(0) = [{}^F p_y, \theta_F, V, \gamma, \beta, a_x, a_y] = [0.5, 0.0, 3.0, 0.0, 0.0, 0.0, 0.0]$. The parameters in Table.II are used in both cases with/without the steering input. The simulations were done using the Intel(R) Core(TM) i7-10700 CPU @ 2.90GHz, RAM 24.0 GB.

TABLE III
PARAMETERS IN SIMULATION WITH STEERING INPUT

S_f	diag $[0, 0, 1, 10^{-3}, 10^{-7}, 10^{-3}, 10^{-3}]$
Q	diag $[7.5, 0.5, 1, 10^{-8}, 10^{-7}, 10^{-3}, 10^{-3}]$
R	diag $[0.0, 10^{-5}, 10^{-5}, 10^{-5}, 10^{-5}]$
R'	diag $[0.1, 10^{-5}, 10^{-5}, 10^{-5}, 10^{-5}]$
δ_{max}	30 [deg]
T_{max}	1000[Nm]

TABLE IV
PARAMETERS IN SIMULATION WITHOUT STEERING INPUT

S_f	diag $[0, 0, 1, 10^{-3}, 10^{-7}, 10^{-3}, 10^{-3}]$
Q	diag $[7.5, 0.5, 1, 10^{-8}, 10^{-7}, 10^{-3}, 10^{-3}]$
R	diag $[0, 5\times10^{-8}, 5\times10^{-8}, 5\times10^{-8}, 5\times10^{-8}]$
R'	diag $[0.1, 10^{-4}, 10^{-4}, 10^{-4}, 10^{-4}]$
δ_{max}	0 [deg]
T_{max}	1000[Nm]

B. Obstacle avoidance simulation with steering input

First, obstacle avoidance with steering input is tested using the parameters listed in Table.III. In this scenario, the vehicle successfully avoided the obstacles. See Fig. 6 to check the simulation result. Basically, the vehicle turned itself using steering input. The torque inputs were mainly used to accelerate the car to follow the reference velocity. This is because steering input has a greater influence on the vehicle motion, and is more effective in reducing the penalty in terms of the cost function. However, right tire torques are slightly larger than left ones where the vehicle is right in front of the obstacle A. This means that torque distribution also contributes to generate yaw-moment of the vehicle, especially in severe situations where it is difficult to make a turn by steering input alone.

C. Obstacle avoidance simulation without steering input

Next, obstacle avoidance without steering input is tested setting parameters in Table.IV. The vehicle was successful in avoiding collisions even though steering input is always zero as shown in Fig.7. Comparing the results between Fig.6 and Fig.7, much higher torque input was needed to avoid collision without steering input. This is a natural way to change the direction of the vehicle, and it is possible to use the torque of each tire completely and skillfully it can be seen

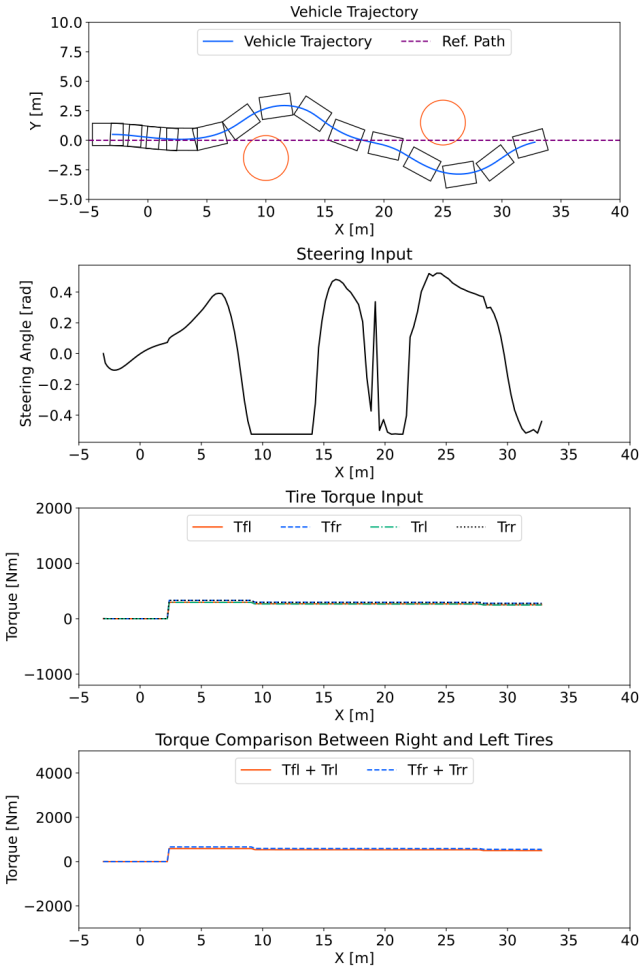

Fig. 6. Obstacle Avoidance (With Steering Input)

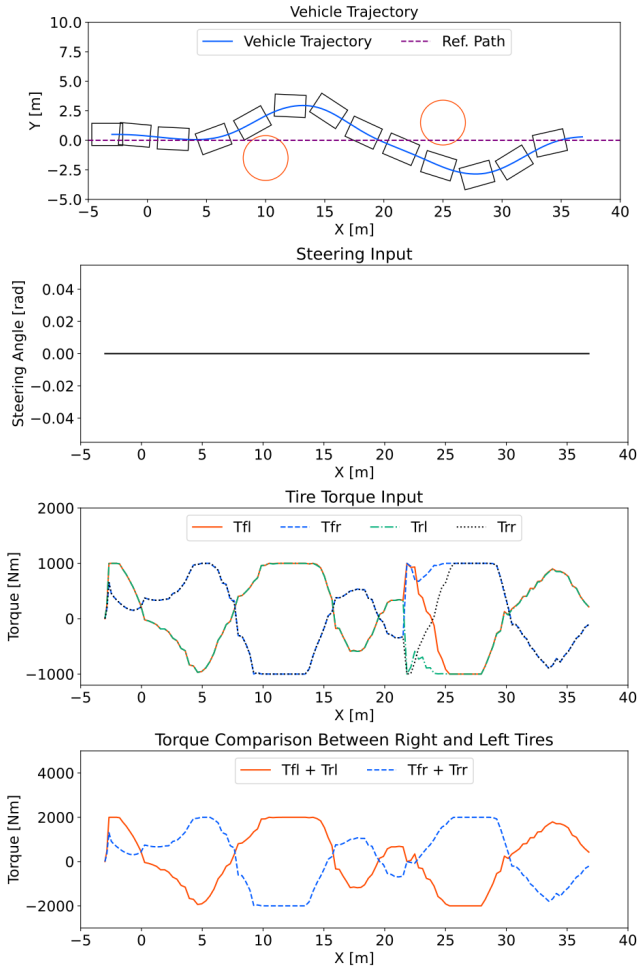

Fig. 7. Obstacle Avoidance (Without Steering Input)

that obstacle avoidance is realized with torque distribution alone. Since the turning performance is reduced when turning without steer, the closest distance from the obstacle is smaller than in the case with normal steering input. The bottom figure in Fig. 7 is helpful to grasp how the torque allocation contributes to the vehicle motion. If the torque generation of the left tires are larger, the vehicle gets yaw-moment to turn right, and the opposite is also true (See Fig.8.) The larger the difference in torque generated by the left and right tires, the larger the rotational moment given to the car.

D. Discussion

The proposed scheme of this study was confirmed to be suitable to achieve obstacle avoidance behavior with/without steering input. While there are several controllers proposed to consider the torque allocation in rule-based manners, our scheme is beneficial because there is no need to prepare another controller to switch the turning on/off steering input; instead, it is achieved by changing the δ_{max} constraint. One of the major advantages of using MPC is that there is no need to prepare a reference trajectory planned to avoid obstacles. Hence, adding another obstacle on the road is also easy; this scheme is flexible and can be expanded to complex roadway conditions. While NMPC is expected to achieve high performance in many cases, handling complex prediction models often leads to a higher computational cost. This study solved this problem by introducing a relatively new optimization solver named PANOC, and achieved to run the simulation in real-time. Fig.9 shows the computation time of the simulations. In both scenarios, the calculation time is much smaller than the control interval 0.05 [s] (See Fig. 9.)

On the other hand, there remains some issues to be solved. See steering input result in the Fig. 6. A sudden change of the steering input was observed at around $X = 19$ [m], where the vehicle faces the obstacle B. Theoretically, this phenomenon could be solved by increasing the length of the prediction horizon. However, extension of the prediction horizon increases the difficulty of the optimization. Achieving a system that works stably while making long predictions is an issue to be overcome in the future.

This study focuses on the obstacle avoidance behavior and fail-safe operation in a case of steering failure, other tasks such as reducing the energy consumption and improving riding comfort is considered to be applicable as a mean of utilizing redundancy. Achieving these goals is a topic for

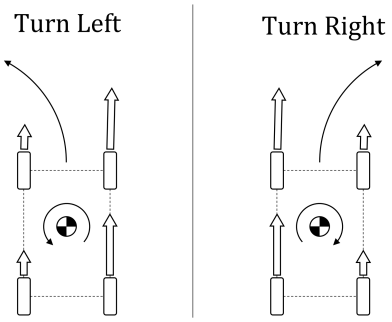

Fig. 8. Vehicle Turn with Torque Distributions

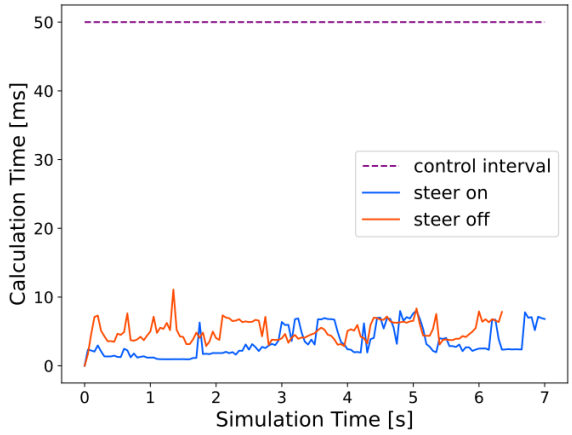

Fig. 9. Computation Time

future research.

V. CONCLUSIONS

This study proposed a scheme to exploit the maximum performance of EV-IWM. It is based on a nonlinear MPC to accurately consider complex vehicle dynamics. Generally, the application of NMPC for this system is limited by computation costs that are too heavy for practical use. However, we introduced an optimization solver referred to as PANOC and achieved real-time control. The simulations of the obstacle avoidance were successful in both cases with and without steering input. These results indicate that the redundancy of EV-IWM contributes significantly to safe driving in the context of facilitating emergency avoidance in a steering failure situation. In the future, other tasks such as energy-efficient driving or the improvement of riding comfort will be achieved by making the best use of the vehicle's flexibility.

REFERENCES

[1] S. Wen and L. Wang, "A study on obstacle avoidance for mobile robot based on fuzzy logic control and adaptive rotation," in Proceedings of the 10th World Congress on Intelligent Control and Automation, 2012, pp. 753–757.

[2] C. Geng, L. Mostefai, M. Denai, and Y. Hori, "Direct yaw-moment control of an in-wheel-motored electric vehicle based on body slip angle fuzzy observer," IEEE Transactions on Industrial Electronics, vol. 56, no. 5, pp. 1411–1419, 2009.

[3] S. Yim, "Fault-tolerant yaw moment control with steer — and brake-by-wire devices," International Journal of Automotive Technology, vol. 15, p. 463–468, 2014.

[4] M. Mostavi, M. Shariatpanahi, and R. Kazemi, "An optimal four wheel steering vehicles control based on pole placement method," WSEAS Transaction on Control and System Theory, Paper Number 487-756, 01 2004.

[5] C. Chatzikomis, A. Sorniotti, P. Gruber, M. Zanchetta, D. Willans, and B. Balcombe, "Comparison of path tracking and torque-vectoring controllers for autonomous electric vehicles," IEEE Transactions on Intelligent Vehicles, vol. 3, no. 4, pp. 559–570, 2018.

[6] S. Taherian, U. Montanaro, S. Dixit, and S. Fallah, "Integrated trajectory planning and torque vectoring for autonomous emergency collision avoidance," in 2019 IEEE Intelligent Transportation Systems Conference (ITSC), 2019, pp. 2714–2721.

[7] A. Muraleedharan, H. Okuda, and T. Suzuki, "Real-time implementation of randomized model predictive control for autonomous driving," IEEE Transactions on Intelligent Vehicles, pp. 1–1, 2021.

[8] M. Aoki, K. Honda, H. Okuda, and T. Suzuki, "Comparative study of prediction models for model predictive path- tracking control in wide driving speed range," in 2021 IEEE Intelligent Vehicles Symposium (IV), 2021, pp. 1261–1267.

[9] K. Kazuki, N. Kenichiro, and S. Kazuma, "Real-time model predictive obstacle avoidance control for vehicles with reduced computational effort using constraints of prohibited region," Mechanical Engineering Journal, vol. 2, no. 3, pp. 14–00 568–14–00 568, 2015.

[10] H. Okuda, N. Sugie, and T. Suzuki, "Realtime collision avoidance control based on continuation method for nonlinear model predictive control with safety constraint," in 2017 11th Asian Control Conference (ASCC), 2017, pp. 1086–1091.

[11] R. Rajamani, Vehicle dynamics and control. Springer Science & Business Media, 2011.

[12] M. Abe, Automotive Vehicle Dynamics. Tokyo Denki University Press, 2008.

[13] S. Tadashi, H. Tomoyuki, and M. Yoshihiro, "Vehicle motion control under limit state and fastest speed control by using nonlinear model predictive control," Transactions of the Society of Instrument and Control Engineers, vol. 53, no. 7, pp. 385–397, 2017.

[14] R. Bingtao, C. Hong, Z. Haiyan, and Y. Lei, "Mpc-based yaw stability control in in-wheel-motored ev via active front steering and motor torque distribution," Mechatronics, vol. 38, pp. 103–114, 2016.

[15] L. Stella, A. Themelis, P. Sopasakis, and P. Patrinos, "A simple and efficient algorithm for nonlinear model predictive control," in 2017 IEEE 56th Annual Conference on Decision and Control (CDC), 2017, pp. 1939–1944.

[16] M. Sampei, "A control strategy for a class of nonholonomic systems - time-state control form and its application," in Proceedings of 1994 33rd IEEE Conference on Decision and Control, vol. 2, 1994, pp. 1120–1121 vol.2.

[17] M. Sampei, H. Kiyota, H. Koga, and M. Suzuki, "Necessary and sufficient conditions for transformation of nonholonomic system into time-state control form," in Proceedings of 35th IEEE Conference on Decision and Control, vol. 4, 1996, pp. 4745–4746 vol.4.

[18] S. Koji, S. Naoki, N. Kenichiro, and S. Kazuma, "Model predictive obstacle avoidance control for vehicles with automatic velocity suppression using artificial potential field," IFAC-PapersOnLine, vol. 51, no. 20, pp. 313–318, 2018, 6th IFAC Conference on Nonlinear Model Predictive Control NMPC 2018.

[19] P. Sopasakis, E. Fresk, and P. Patrinos, "Open: Code generation for embedded nonconvex optimization," IFAC-PapersOnLine, vol. 53, no. 2, pp. 6548–6554, 2020, 21st IFAC World Congress.

[20] Y. Yoon, J. Shin, H. J. Kim, Y. Park, and S. Sastry, "Model-predictive active steering and obstacle avoidance for autonomous ground vehicles," Control Engineering Practice, vol. 17, no. 7, pp. 741–750, 2009.